

## SEPARATION OF GLUCOSE AND FRUCTOSE USING A SEMI-CONTINUOUS CHROMATOGRAPHIC REFINER WITH AND WITHOUT A PURGE COLUMN

Kwang-Nam Lee<sup>†</sup>, Chang-Yong Lee\* and Won-Kook Lee\*\*

Central Research Institute, Dongsung Chemical Co., Ltd., 419-1, Chung-ree, Kusung-myun, Kyungki-do 449-910, Korea

\*Department of Industrial Chemistry, Cheonan National Technical College, Cheonan 330-240, Korea

\*\*Department of Chemical Engineering, Korea Advanced Institute of Science and Technology, Taejon 305-701, Korea

(Received 17 June 1995 • accepted 26 September 1995)

**Abstract**—The separation of an aqueous mixture of glucose and fructose was experimentally performed by using a semi-continuous chromatographic refiner (SCCR) which consists of purge, pre-feed and post-feed section. Packing materials were Ca<sup>2+</sup> ion form of DOWEX 50W 12X resin and water was used as an isocratic eluent. The plug flow model with velocity dependent mass transfer resistance was presented for calculating both products and on-concentrations in the SCCR unit. The effects of factors - the ratio of adsorbed phase to mobile phase flow rate,  $\alpha$  (margin), purge rate and total number of columns in the SCCR operation - were studied and the validity of the model was experimentally confirmed. The modified SCCR operation without a purge section was also studied.

*Key words: Glucose, Fructose, Separation, SCCR, Purge Column, Ion Exchange*

### INTRODUCTION

The separation of materials that are produced as mixtures in bioprocessing is necessary to successful operation. When starch is hydrolyzed to produce glucose and glucose is partially isomerized by isomerase enzymes, the syrup thus produced contains 71% sugar solids of which 50% w/w is glucose, 42% w/w fructose and 8% w/w higher saccharides. The proportion of fructose in this syrup is then increased to 55-90% w/w to produce a sweetener marketed as High Fructose Corn Syrup. The glucose-fructose separation is an industrially significant in successful operation of bioprocessing and the continuous chromatographic method contributes significantly to the progress. The processes which have been the most successful to separation of glucose-fructose mixture are the simulated counter current moving bed chromatographic separators. In such systems an effective counter current operation is achieved by the sequential periodic movement of feed and exit ports through a series of fixed beds in the direction of fluid flow. Because of this periodic counter current action, the adsorbent is used very effectively in this process. These processes can be divided into two types. One is the "SORBEX" family of processes developed by UOP [Broughton, 1968], and the other is the semi-continuous chromatographic refiner (SCCR) developed by Barker et al. [1984]. The useful and comprehensive review of these two types has been given by Ruthven and Ching [1989]. Recently, the simulated counter-current moving bed system is developed to a device for carrying out chemical reaction and separation simultaneously by Tonkovich and Carr [1994a, 1994b] and Ray et al. [1994]. Otherwise in the SORBEX type, the products cannot be obtained continuously within a switch time in the SCCR unit. Thus in SCCR unit, an effective mathematical model to predict both products and on-concentrations is needed to obtain the products effectively. However, it seems that little study has been done on the model equation of the SCCR unit [Ching and Ruthven,

1985; Barker and Thawait, 1983; Barker and Ganetsos, 1987]. The purpose of this work described here is to suggest the model which can predict the performance of the SCCR unit and test the possibility of operation of the SCCR unit and test the possibility of operation of the SCCR unit without a purge column. In all experiments, the operating temperature was maintained to 50°C to reduce the viscosity and maintain the pressure drop within acceptable limits.

### OPERATION PRINCIPLE OF THE SCCR UNIT

The counter-current movement is simulated by sequencing a system of inlet and outlet port functions around the 12 stainless steel columns. Each of these columns was packed with a calcium charged DOWEX 50W 12X resin. Fig. 1 illustrates the operation principle of the SCCR unit for separation of glucose-fructose mixture. In (A) the feed enters column 7. The less strongly adsorbed glucose moves with the eluent (distilled water), which enters the system at column 2 and exits with glucose from column 12. The fructose, the strongly adsorbed component due to the formation of a chemical complex with Ca<sup>2+</sup>, is preferentially retained by the resin. After a switch time, the position of the inlet and outlet port is advanced by one column as shown in (B) and (C). This simulation has the same effect of the movement of fructose with the stationary phase. At the end of 12 such switches, when each column has served as a purge entry, eluent entry, glucose exit and feed column, a cycle is completed. After a number of cycles, a pseudo-equilibrium state is reached as the shape of the glucose and fructose profile becomes uniform and reproducible from cycle to cycle.

### DESCRIPTION OF THE EQUIPMENT

The equipment was made up of twelve 1-cm-diameter stainless steel columns with packed length of 30 cm linked alternately top and bottom to form a closed loop. The upper and lower bed sup-

<sup>†</sup>To whom correspondences should be addressed.

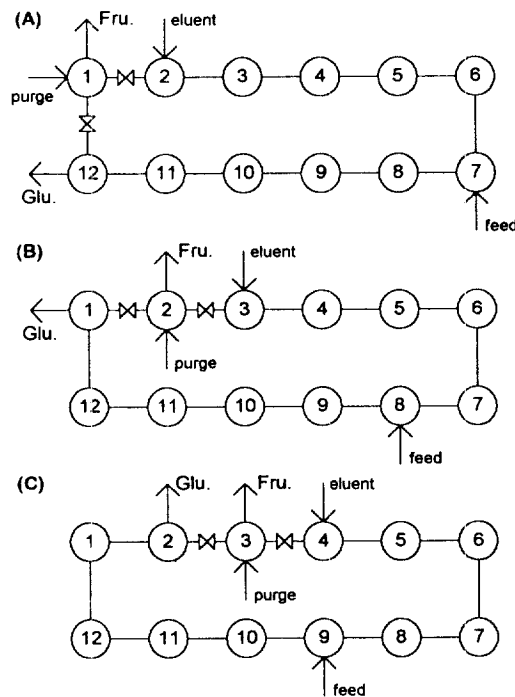


Fig. 1. Operation principle of the SCCR unit.

ports consisted of two layer of fine mesh stainless steel screen. Three specially designed distributors which each has one inlet and 12 outlets were used to control purge, eluent and feed inlet. Fig. 2 shows the configuration of three columns out of 12 columns in which two three-way valves and one on-off valve were located on each column. One three-way valve was for eluent or purge inlet from each distributor, and the other was for glucose-rich or fructose-rich products and transfer line to the next column. These lines were as short as possible so as to reduce the effects of dispersion and residence time between columns. One on-off valve was used only as the feed inlet from the distributor. All columns were surrounded by a constant temperature enclosure.

## CHROMATOGRAPHIC MEASUREMENTS

In order to characterize the equilibrium and kinetic properties of the adsorbent, a series of chromatographic measurements was carried out at 50°C on 12 of the columns. Using the dispersed plug flow model and Gluekauf's linear driving force approximation, the means and variances of the response peaks were calculated according to the usual expression.

$$t = \int_0^x c dt / \int_0^x c dt \quad (1)$$

$$\sigma^2 = \int_0^x c(t - \bar{t})^2 dt / \int_0^x c dt \quad (2)$$

For a linear system the mean retention time is related to the adsorption equilibrium constant by:

$$\bar{t} = \frac{L}{v} \left( 1 + \frac{1 - \epsilon}{\epsilon} K \right) \quad (3)$$

The chromatographic HETP is also given by:

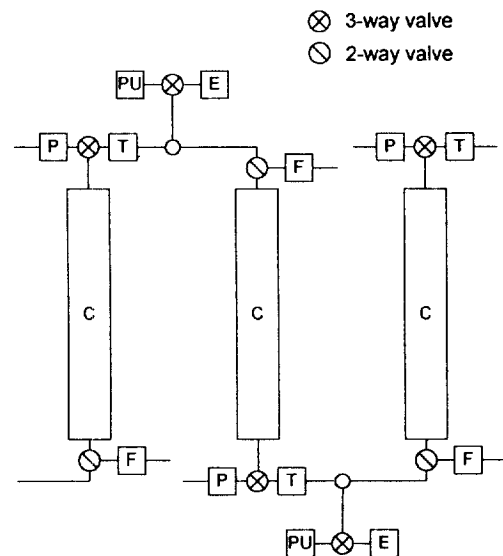


Fig. 2. Schematic arrangement of columns and valves.

C: column, PU: purge line, E: eluent line, P: product line, F: feed line, T: transfer line.

$$\begin{aligned} \text{HETP} &= \frac{\sigma^2}{\bar{t}^2} L \\ &= 2 \frac{D_L}{v} + 2v \left( \frac{\epsilon}{1 - \epsilon} \right) \frac{1}{K} \frac{1}{k} \left[ 1 + \frac{\epsilon}{(1 - \epsilon) K} \right]^{-2} \end{aligned} \quad (4)$$

where  $k$  is the effective overall mass transfer coefficient, defined by:

$$\frac{\partial q}{\partial t} = k(q^* - q) = k(Kc - q) \quad (5)$$

Blue dextran, which because of its size (molecular weight = 2,000,000) does not penetrate into the resin was used as a tracer to estimate the void fraction,  $\epsilon$ , and the value obtained from its mean retention time was 0.372. Values of  $\bar{t}$  for both the glucose and fructose are plotted against  $(L/v)$  and shown in Fig. 3(a). The equilibrium constants for glucose and fructose ( $K_G = 0.123$ ,  $K_F = 1.310$ ) are obtained from the slopes. The axial dispersion in a liquid system is proportional to the flow rate [Ghim and Chang, 1982; Ruthven, 1984]:

$$D_L = \eta v d \quad (6)$$

Since the value  $D_L/v$  may be constant and can be calculated from the intercept of HETP vs.  $v$  of Fig. 3(b). The effective overall mass transfer coefficients can be calculated from the slope of the same plot with the known values of equilibrium constants. But if the axial dispersion effect is negligible, the effective overall mass transfer coefficient can be described by the velocity dependence:

$$k(v) = \frac{av}{v + b} \quad (7)$$

The above two models are compared in Table 1. The adsorption rate constant of glucose is greater than that of fructose. Fructose is chemically complexed by the  $\text{Ca}^{2+}$  ion in the resin, whereas glucose is only very weakly adsorbed. The difference in the adsorption rate constant may be attributed to the finite rate of for-

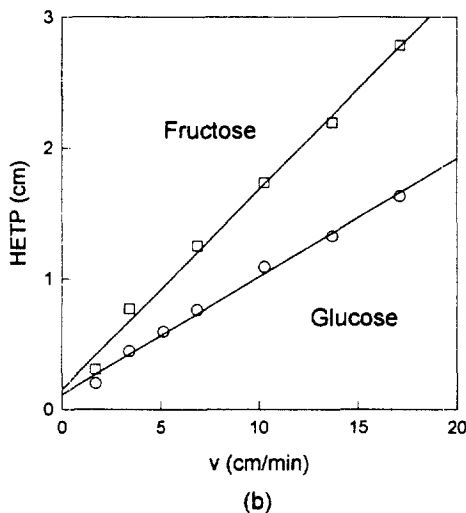
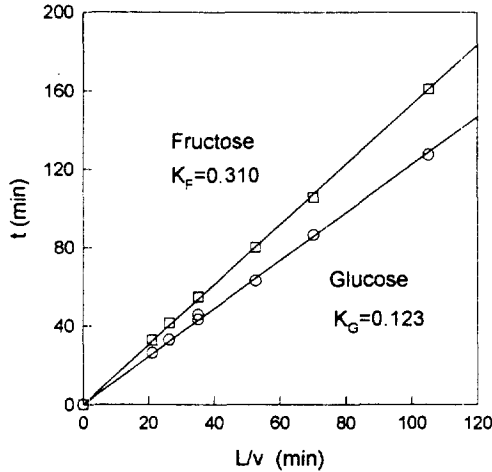


Fig. 3. (a) mean retention time plotted against (L/v), (b) HETP as a function of fluid velocity.

mation of the fructose complex. The comparison of two models with experimental values are shown in Fig. 4. There is no difference between two models. This may be explained by which the axial dispersion effect is lumped to the overall mass transfer resistance depending on the velocity.

**MATHEMATICAL TREATMENT OF THE SCCR UNIT**

In the SCCR unit, each adsorption column can be considered to be a fixed bed except at the moment of moving purge, eluent and feed column. Because the plug flow model with velocity dependent overall mass transfer resistance well describe the chro-

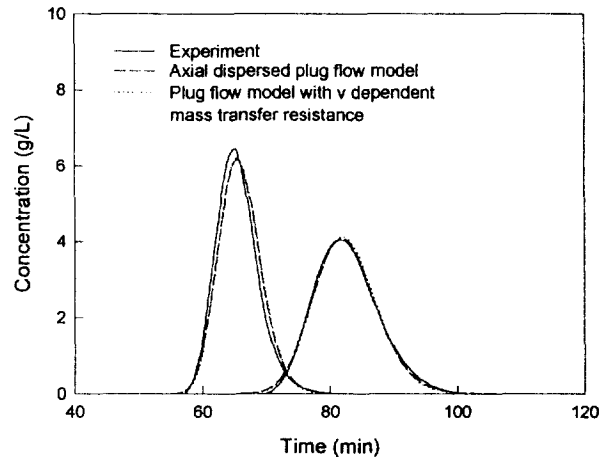


Fig. 4. Comparison of experimental and theoretical curves of two model when volumetrical flow rate is 2 cc/min.

matographic responses, mass balance equations with respect to the concentrations of mobile phase *c* and the stationary phase *q* and the boundary condition at column exit can be given by Eqs. (8)-(10), which are set to positive for the direction of liquid flow:

$$\frac{\partial c_i}{\partial t} = -v \frac{\partial c_i}{\partial z} - \frac{1-\epsilon}{\epsilon} k(v_i)(Kc_i - q_i) \tag{8}$$

$$\frac{\partial q_i}{\partial t} = k(v_i)(Kc_i - q_i) \tag{9}$$

$$\frac{\partial c_i}{\partial z} = 0 \text{ at } z = L \tag{10}$$

where the subscript *i* refers to the column number (1 to 12). The following conditions are written for the inlet points between columns when feed enters column 7:

At the inlet point of the purge stream

$$c_{1,0} = 0.0 \tag{11}$$

At the inlet point of the eluent columns

$$c_{2,0} = 0.0 \tag{12}$$

At the inlet point of the feed stream

$$c_{7,0} = \frac{v_6 c_{6,1} + v_7 c_7}{v_7} \tag{13}$$

At the inlet points of other columns

$$c_{i,0} = c_{i-1,1} \text{ (} i = 3, \dots, 6, 8, 12 \text{)} \tag{14}$$

where the first subscript is the column number and the second subscript denotes the inlet (0) and outlet (1) of the liquid stream

**Table 1. Comparison of two models**

|  | Axial dispersed plug flow model with constant mass transfer resistance |          | Plug flow model with velocity dependent mass transfer resistance |                     |
|--|--|----------|--|---------------------|
|  | Glucose  | Fructose | Glucose  | Fructose            |
| Axial dispersion coefficient (cm <sup>2</sup> /min)              | 0.057v   | 0.077v   | -  | -                   |
| Effective overall mass transfer coefficient (min <sup>-1</sup> ) | 3.155  | 2.941    | $\frac{3.155v}{v+1.315}$   | $\frac{2.94v}{v+1}$ |

in each column.

Under the assumption that the components do not interact in the linear isotherm, the numerical solution of the transient model of each fixed bed was performed through the orthogonal collocation method [Finlayson, 1980; Villadsen and Michelson, 1980] which reduces the original partial differential equations to a set of ordinary differential equations. These differential equations were integrated through a fourth order Runge-Kutta method and selection of seven collocation points at each fixed bed gave sufficient precision to calculate the theoretical profiles under the experimental conditions of this work. The details of the calculation procedure are described in earlier publications by the authors [Lee and Lee, 1992]. With the integration method, the pseudo-equilibrium concentration profile can be calculated.

### EXPERIMENTAL

The feed solution used in the SCCR unit contained 10 g/L each of glucose and fructose dissolved in distilled water. Liquid samples were taken from the exit of each column and analyzed by HPLC (Waters Co.) using a "Aminex 87C" column (Biorad Co.). The stainless steel analytical column is 4 mm in diameter and 250 mm in length. The packing consists of 9  $\mu$ m sulfonated divinyl benzene-styrene beads in the  $Ca^{2+}$  form. Elution was performed at 85°C at a fluid (distilled water) velocity of 0.4 cc/min. Under these conditions the retention time for the glucose and fructose peaks were 4.3 and 5.5 min, respectively. All runs in the SCCR unit were carried out at 50°C and samples were taken as close as possible to the end of the switch interval for on-concentrations and split into 10 parts in the given switch time for the glucose- and fructose-rich products.

### RESULTS AND DISCUSSION

It was noted in the operation principle of the SCCR unit that the packing of the column is moved counter-current to the direction of mobile phase flow at a correct rate; that is, the slow moving component can be made to travel with the packing and the fast moving component with the mobile phase. Thus, the required flow condition may be conveniently specified in term of the dimensionless parameter  $\gamma[(1-\epsilon)Ku/\epsilon v]$ , which is the ratio of the downward flow in the adsorbed phase to the upward flow in the mobile phase.

$$\begin{aligned} \text{pre-feed section } \gamma_G < 1.0, \gamma_F > 1.0 \\ \text{post-feed section } \gamma_G < 1.0, \gamma_F > 1.0 \end{aligned} \quad (15)$$

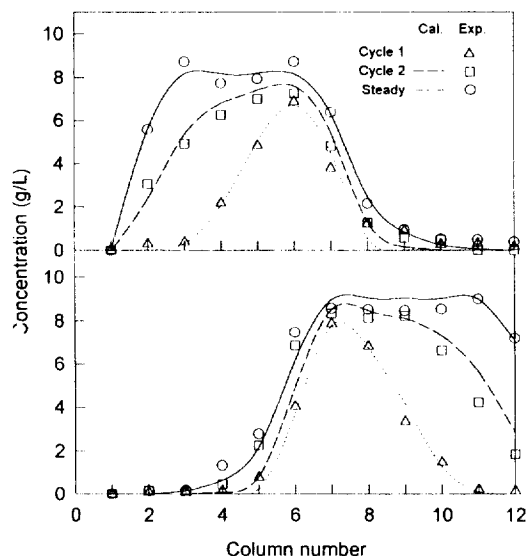


Fig. 5. Experimental and theoretical transient concentration profiles of Run 2 at the end of a switch time. Total of 12 columns, each 30 cm long.

Knowing the limiting adsorption equilibrium constants  $K_G$  and  $K_F$ , these inequalities can be translated into two equations relating the flow rate ratios, E/S, F/S and the parameter  $\alpha (>1.0)$  by which the inequalities are satisfied.

$$\begin{aligned} \text{pre-feed section } E/S = K_G \alpha \\ \text{post-feed section } E/S + F/S = K_F / \alpha \end{aligned} \quad (16)$$

For each section of the SCCR unit, Eq. (16) in terms of four variables E, S, F and  $\alpha$  is given. Thus, by specifying two variables, the other two variables can be obtained. Here we simply specify the switch time, which determines the variable S, and the parameter  $\alpha$  is fixed to a 10% margin to define the eluent (E) and the feed flow rate (F).

In a purge section, excess flow is needed only to wash out the tracer within a switch time:

$$\text{purge section } \gamma_F < 1.0 \quad (17)$$

Sometimes this excess flow may cause the dilution of the product, so that some trials are needed to determine the proper purge rate. Because each column contains the eluent phase in the void volume, this amount has to be compensated for in the eluent rate to get the actual eluent rate in an SCCR unit.

Table 2. Experimental Conditions of SCCR operation

|                        | Run no. | Switch time (min) | Eluent rate (cc/min) | Feed rate (cc/min) | Purge rate (cc/min) | $\gamma_G$ |           | $\gamma_F$ |           | Purge section | $\alpha$ |
|------------------------|---------|-------------------|----------------------|--------------------|---------------------|------------|-----------|------------|-----------|---------------|----------|
|                        |         |                   |                      |                    |                     | pre-feed   | post-feed | pre-feed   | post-feed |               |          |
| With a purge column    | 1       | 3                 | 0.67(3.60)           | 0.72               | 7.0                 | 0.91       | 0.44      | 2.28       | 1.10      | 0.22          | 1.1      |
|                        | 2       | 3                 | 0.67(3.60)           | 0.72               | 5.0                 | 0.91       | 0.44      | 2.28       | 1.10      | 0.22          | 1.1      |
|                        | 3       | 3                 | 0.67(2.70)           | 0.72               | 3.0                 | 0.91       | 0.44      | 2.28       | 1.10      | 0.22          | 1.1      |
|                        | 4       | 4                 | 0.50(2.70)           | 0.54               | 5.0                 | 0.91       | 0.44      | 2.28       | 1.10      | 0.23          | 1.1      |
|                        | 5       | 3                 | 0.73(3.65)           | 0.54               | 5.0                 | 0.83       | 0.48      | 2.09       | 1.10      | 0.31          | 1.2      |
|                        | 6       | 6                 | 0.67                 | 0.72               | 5.0                 | 0.91       | 0.44      | 2.28       | 1.10      | 0.31          | 1.1      |
| Without a purge column | 7       | 3                 | 0.67(3.60)           | 0.72               | 4.32                | 0.91       | 0.44      | 2.28       | 1.10      | -             | 1.1      |
|                        | 9       | 6                 | 0.67(3.60)           | 0.72               | 4.32                | 0.91       | 0.44      | 2.28       | 1.10      | -             | 1.1      |

Values in parentheses are the actual flow rate according to Eq. (10).

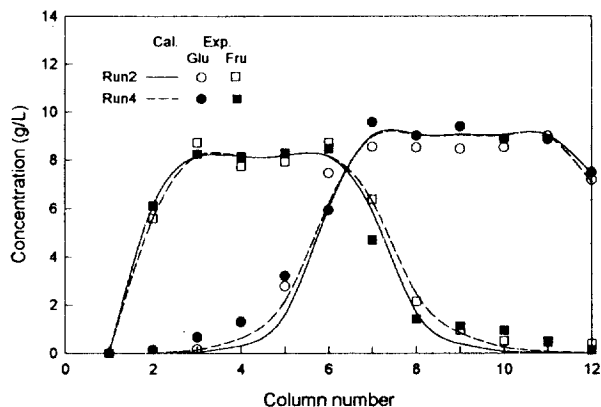


Fig. 6. Comparison of experimental and theoretical concentration profiles Run 2 and Run 4 at the end of a switch time. Total of 12 columns, each 30 cm long.

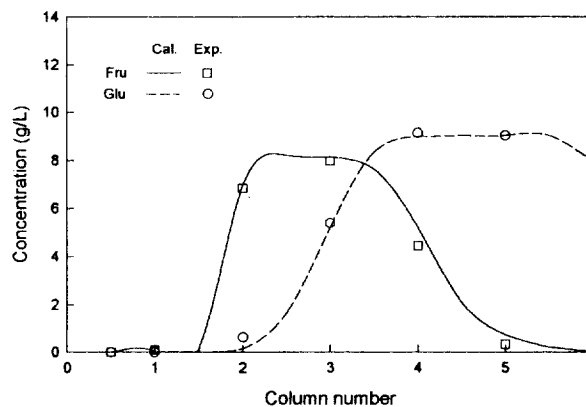


Fig. 8. Experimental and theoretical concentration profiles of Run 6 at the end of a switch time. Total of 6 columns, each 60 cm long.

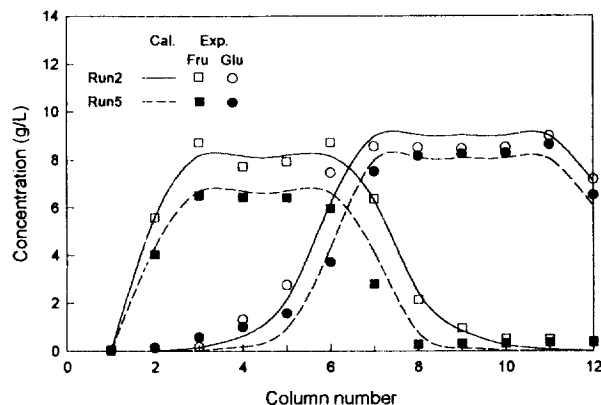


Fig. 7. Comparison of experimental and theoretical concentration profiles of Run 2 and Run 5 at the end of a switch time. Total of 12 columns, each 30 cm long.

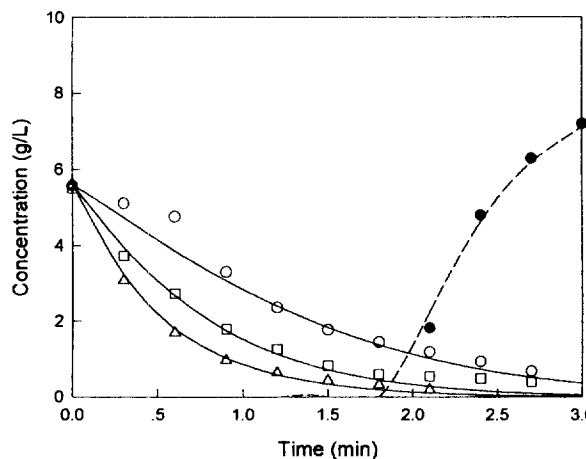


Fig. 9. Experimental and theoretical concentration profiles of glucose (at 12th column; cal. ---, exp. ●) and fructose-rich product [at purge column; cal. —, exp. ○ (Run 1), □ (Run 2), △ (Run 3)].

$$E' = E + A\epsilon u \quad (18)$$

Steady state concentration profiles were measured under the eight sets of operating conditions summarized in Table 2 and the required flow rates were obtained from Eq. (16) and (18).

### 1. SCCR Operation with a Purge Column

The transient and steady state response of an SCCR operation are shown in Fig. 5 together with the theoretical profiles calculated from the rate model. Theoretical curves provide a reasonably good representation of the experimental profiles. Although this would normally be operated under quasi-state conditions, the knowledge of the transient behavior of the system is important in relation to start-up. Fig. 6 shows the effects of ratio of hypothetical adsorbed phase to mobile phase flow rate. Although flow conditions of Run 2 differ from those of Run 4, similar profiles can be obtained with the same flow ratios (same  $\gamma$  values). The small difference between the theoretical profiles seems to be due to the velocity dependent kinetic parameter.

When  $\alpha$  is increased with a fixed  $S$  (that is, fixed switch time), it has the same effect of increasing the eluent rate and decreasing the feed flow rate according to Eq. (16). The meaning of Eq. (16) is the slope of operating line in the McCabe-Thiele diagram for the operation of counter-current adsorption. Thus, when  $\alpha$  is increased, the slope of the operating line in pre-feed section is in-

creased and that in the post-feed section decreased. This effect reduces the required NTP but results in more dilution of the product. This is well illustrated in Fig. 7.

With sufficiently small elemental beds switched with appropriate frequency, such a system indeed becomes a perfect analog of a counter-current flow system. However, it has been shown both theoretically and experimentally that most of the benefit of counter-current flow can be achieved by a rather modest degree of subdivision of the bed [Liapis and Rippin, 1979]. Thus it is of interest to investigate the number of total columns used in the SCCR unit with regard to the complexity of the operation and the cost of the equipment. In Run 6, a total of 6 columns, each 60 cm long, was used in operating the unit, and the eluent and feed rate were the same as in Run 2 but the switch time. The results of simulation and experiment (Fig. 8) tell us the possibility of an SCCR operation with 6 columns under the given column length of 360 cm. Thus there is no need to operate with twelve columns. The effects of purge rates were tested while maintaining other flow rates constant (Run 1, 2 and 3). Because the profiles of fructose and glucose rich products can be accurately estimated as shown in Fig. 9 and 10, substantial dilution

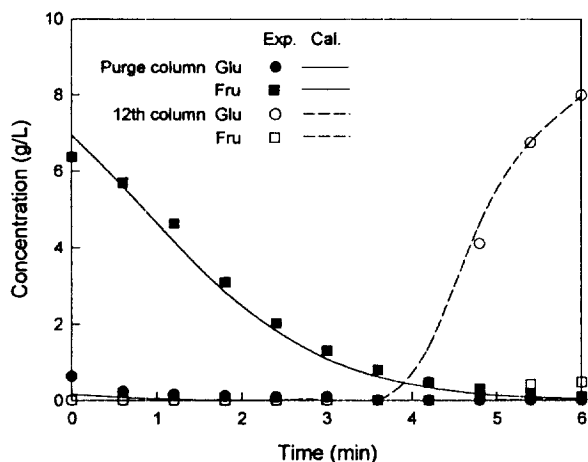


Fig. 10. Experimental and theoretical concentration profiles of glucose- and fructose-rich product (Run 6).

of the product can be avoided when the collection times of the products are properly selected. Here, the 'critical' dilution was arbitrarily defined as that value where the product concentration was about 10% of the feed concentration. In all experiments, the fructose-rich products above the 'critical' dilution were collected and the glucose-rich products were collected as soon as the glucose started to exit. The experimental results of these techniques are summarized in Table 3 and 4, respectively. In Run 3, the purge rate, 3 cc/min, seemed not enough to strip the fructose within a switch time (see Fig. 9). But in all experiments, because the fructose below the 'critical' dilution was discarded and the glucose was collected when it started to exit, it was possible to

Table 3. Experimental results in the fructose-rich product

|                        | Run no. | Switch time (min) | Eluent rate (cc/min) | Product collection time (min) | Average conc. (g/L) | Purity (%)    | Recovery (%)  |
|------------------------|---------|-------------------|----------------------|-------------------------------|---------------------|---------------|---------------|
| With a purge column    | 1       | 3                 | 7.0                  | 0 to 0.9                      | 2.69 (2.70)         | 97.73 (99.92) | 78.46 (81.38) |
|                        | 2       | 3                 | 5.0                  | 0 to 1.2                      | 2.91 (2.94)         | 96.38 (99.92) | 80.83 (81.67) |
|                        | 3       | 3                 | 3.0                  | 0 to 2.1                      | 3.16 (2.94)         | 96.98 (99.92) | 92.17 (85.75) |
|                        | 4       | 4                 | 5.0                  | 0 to 1.6                      | 3.28 (3.06)         | 97.05 (100.0) | 91.11 (85.00) |
|                        | 5       | 3                 | 5.0                  | 0 to 0.9                      | 2.74 (2.64)         | 92.68 (100.0) | 76.11 (73.33) |
|                        | 6       | 6                 | 5.0                  | 0 to 1.8                      | 4.30 (4.01)         | 98.44 (98.73) | 89.58 (83.54) |
| Without a purge column | 7       | 3                 | 4.32                 | 0 to 1.5                      | 2.96 (2.79)         | 97.35 (100.0) | 88.71 (83.82) |
|                        | 8       | 6                 | 4.32                 | 0 to 2.4                      | 3.59 (3.74)         | 97.98 (99.07) | 86.04 (89.66) |

Values in parentheses are the theoretical results.

Table 4. Experimental results in the glucose-rich product

|                        | Run no. | Switch time (min) | Eluent rate (cc/min) | Product collection time (min) | Average conc. (g/L) | Purity (%)    | Recovery (%)    |
|------------------------|---------|-------------------|----------------------|-------------------------------|---------------------|---------------|-----------------|
| With a purge column    | 2       | 3                 | 4.32                 | 1.8 to 3.0                    | 4.12 (4.15)         | 95.29 (100.0) | 98.60 (99.37)   |
|                        | 4       | 3                 | 4.32                 | 2.4 to 4.0                    | 4.14 (4.26)         | 98.67 (100.0) | 101.92* (99.05) |
|                        | 5       | 3                 | 4.19                 | 1.8 to 3.1                    | 3.79 (3.25)         | 97.68 (100.0) | 117.63* (100.0) |
|                        | 6       | 6                 | 4.32                 | 3.6 to 6.0                    | 3.79 (4.20)         | 93.76 (99.71) | 90.75 (100.0)   |
| Without a purge column | 7       | 3                 | 4.32                 | 1.8 to 3.0                    | 2.96 (2.79)         | 88.71 (92.39) | 104.64* (99.00) |
|                        | 8       | 6                 | 4.32                 | 3.6 to 6.0                    | 3.89 (4.25)         | 92.73 (97.47) | 93.36 (100.0)   |

Values in parentheses are the theoretical results.

\*Values too high due to an analytical inaccuracy.

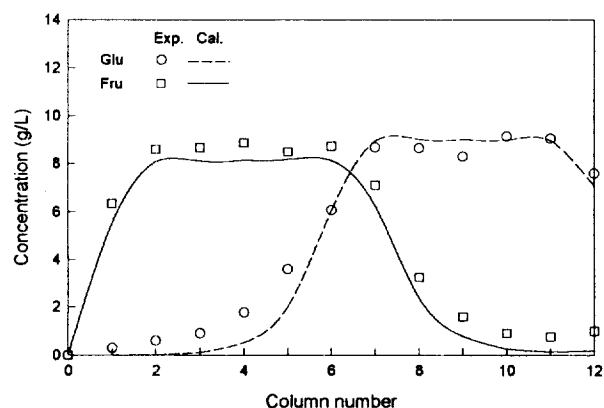


Fig. 11. Experimental and theoretical transient concentration profiles of Run 7 at the end of a switch time, total of 12 columns, each 30 cm long.

strip the fructose-rich product and maintain the purity even with the purge rate mentioned above. Therefore, such purge rate can decrease the eluent requirement and the discarded dilutions can be recycled as eluents to recover all the sugar feeding to the SCCR unit.

## 2. SCCR Operation without a Purge Column

Experience gained on the collection method of both products in the SCCR unit led us to investigate the alternative operating mode in the same unit. As shown in Fig. 1, the isolated purge column containing fructose is purged to obtain fructose-rich product and thereby regenerate the packing ready to receive the glucose of 12th column. But if it is operated without a purge column, fructose remained in the end parts of 1st column at one

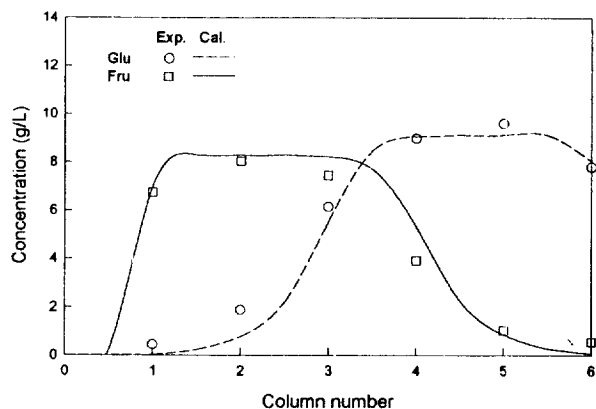


Fig. 12. Experimental and theoretical transient concentration profiles of Run 8 at the end of a switch time, total of 6 columns, each 60 cm long.

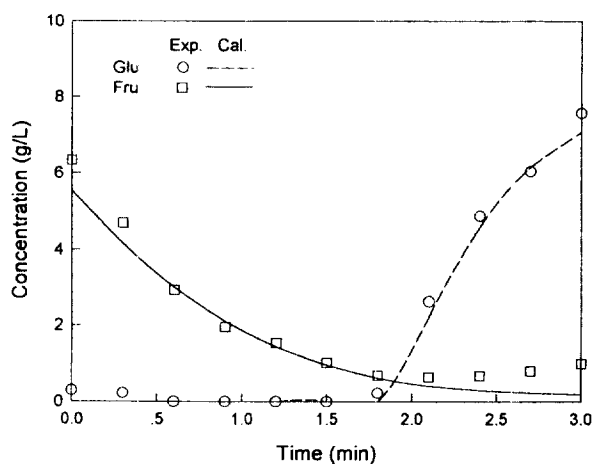


Fig. 13. Experimental and theoretical concentration profiles of glucose- and fructose-rich product (Run 7).

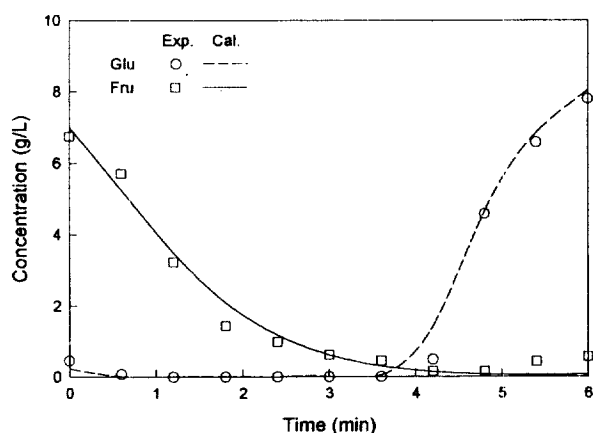


Fig. 14. Experimental and theoretical concentration profiles of glucose- and fructose-rich product (Run 8).

switch interval will be exited with the flow rate of post-feed section (eluent plus feed flow rate) at earlier time of next switch and glucose will be collected at later time of next switch. That is, at the same column (12th column), both products can be obtain-

ed with different time intervals. As shown in Fig. 11 and 12, profiles of on-concentration are more broadened than those obtained from the operation with a purge column. By operating the SCCR unit without a purge column, there are some advantages regarding to the small eluent requirement, the simplicity of operation and the low cost of equipment but at the expense of product purity of the glucose-rich product (Fig. 13 and 14). When Run 7 was compared with Run 8 in product collection of glucose-rich product, the operation with a total of 6 columns under the same total column length (360 cm) was preferred because of longer switch interval with same purge flow rate. In these operations, the same product collection method was applied and the results were also summarized in Table 3 and 4.

## CONCLUSION

The separation of a glucose and fructose mixture by the use of a semi-continuous chromatographic refiner (SCCR) with and without a purge column was performed experimentally. In the SCCR unit, considering each adsorption column to be a fixed bed except at the moment of moving purge, eluent and feed column, the concentration profiles could be represented by the plug flow model with overall effective rate coefficient including axial dispersion effect. The numerical values could be calculated by the orthogonal collocation method. The column switching can be simulated by rearranging the concentrations corresponding to the collocation points backward, by one column, at the end of a switch time. The SCCR operation without a purge column was tried. It was the first time to operate in this mode and possible to obtain the High Fructose Corn Syrup with 55 to 90% fructose. Especially the glucose- and fructose-rich product profiles were accurately predicted, so that the both products could be obtained more efficiently.

## NOMENCLATURE

- A : cross sectional area of column [ $\text{cm}^2$ ]
- a, b : defined in Eq. (7)
- c : fluid phase concentration [ $\text{gL}^{-1}$ ]
- $c_f$  : feed concentration [ $\text{gL}^{-1}$ ]
- d : particle diameter [cm]
- $D_L$  : axial dispersion coefficient [ $\text{cm}^2 \text{min}^{-1}$ ]
- E : eluent flow rate in the counter-current adsorption system [ $\text{cc min}^{-1}$ ]
- $E'$  : actual eluent flow rate in the SCCR unit [ $\text{cc min}^{-1}$ ]
- F : feed flow rate [ $\text{cc min}^{-1}$ ]
- H : height equivalent to one theoretical plate [cm]
- K : adsorption equilibrium constant [ $=q^*/c$ ]
- k : effective overall mass transfer coefficient [ $\text{min}^{-1}$ ]
- L : length of adsorbed bed
- NTP : number of theoretical plate
- q : adsorbed phase concentration [ $\text{gL}^{-1}$ ]
- S : hypothetical adsorbent recirculation rate in equivalent counter current system [ $\text{cc min}^{-1}$ ]
- SCCR : semi-continuous chromatographic refiner
- t : time [min]
- $\bar{t}$  : mean retention time [min]
- u : hypothetical solid velocity ( $=L/\tau$ ) [ $\text{cm min}^{-1}$ ]
- v : interstitial fluid phase velocity [ $\text{cm min}^{-1}$ ]
- $v_f$  : feed velocity [ $\text{cm min}^{-1}$ ]
- X : dimensionless axial distance [ $=z/L$ ]

Z : axial distance in adsorbent bed [cm]

#### Greek Letters

$\alpha$  : margin defined in Eq. (16)  
 $\gamma$  : dimensionless parameter [ $= (1-\epsilon)Ku/\epsilon v$ ]  
 $\epsilon$  : void fraction  
 $\eta$  : scale of axial eddy dispersion  
 $\sigma$  : standard deviation of response peak [min]  
 $\tau$  : switch time [min]

#### Subscripts

F : fructose  
 G : glucose

#### REFERENCES

- Barker, P. E. and Thawait, S., "Separation of Fructose from Carbohydrate Mixtures by Semi-continuous Liquid Chromatography", *Chem. Ind.*, **7**, 817 (1983).
- Barker, P. E., Irlam, G. A. and Abusabah, E. K. E., "Continuous Chromatographic Separation of Glucose-fructose Mixtures Using Anion-exchange Resin", *Chromatographia*, **18**(10), 567 (1984).
- Barker, P. E. and Ganetsos, G., "The Development and Applications of Preparative-scale Continuous Chromatography", *Sep. Sci. Tech.*, **22**, 2011 (1987).
- Broughton, D. B., "Molex: Case History of a Process", *Chem. Eng. Prog.*, **64**(8), 60 (1968).
- Ching, C. B. and Ruthven, D. M., "An Experimental Study of a Simulated Counter-current Adsorption System-I. Isothermal Steady State Operation", *Chem. Eng. Sci.*, **40**(6), 877 (1985).
- Finlayson, B. A., "Nonlinear Analysis in Chemical Engineering", McGraw-Hill (1980).
- Ghim, Y. S. and Chang, H. N., "Adsorption Characteristics of Glucose and Fructose in Ion-exchange Resins Columns", *Ind. Eng. Chem. Fund.*, **21**, 369 (1982).
- Lee, K. N. and Lee, W. K., "A Theoretical Model for the Separation of Glucose and Fructose by Using Semi-continuous Chromatographic Refiner", *Sep. Sci. Tech.*, **27**(3), 295 (1992).
- Lee, K. N. and Lee, W. K., "Separation of Glucose and Fructose at a High Concentration by Using Semi-continuous Chromatographic Refiner", *J. Chem. Eng. Japan*, **25**(5), 533 (1992).
- Liapis, A. I. and Rippin, D. W. T., "Simulation of Binary Adsorption in Continuous Counter-current Operation in Comparison with Other Operating Modes", *AIChE*, **25**, 455 (1979).
- Ray, A. K., Carr, R. W. and Aris, R., "The Simulated Countercurrent Moving Bed Chromatographic Reactor: A Novel Reactor Separator", *Chem. Eng. Sci.*, **49**(4), 469 (1994).
- Ruthven, D. M., "Principle of Adsorption and Adsorption Process", Wiley, NY (1984).
- Ruthven, M. R. and Ching, C. B., "Counter-current and Simulated Counter-current Adsorption Separation Processes", *Chem. Eng. Sci.*, **44**(5), 1011 (1989).
- Tonkovich, A. L. Y. and Carr, R. W., "The Simulated Countercurrent Moving-bed Chromatographic Reactor for the Oxidative Coupling of Methane: Experimental Results", *Chem. Eng. Sci.*, **49**(24A), 4647 (1994a).
- Tonkovich, A. L. Y. and Carr, R. W., "Modeling of the Simulated Countercurrent Moving-bed Chromatographic Reactor Used for the Oxidative Coupling of Methane", *Chem. Eng. Sci.*, **49**(24A), 4657 (1994b).
- Villadsen, J. and Michelson, M. L., "Solution of Differential Equation Models by Polynomial Approximation", Prentice Hall, Englewood Cliffs, NJ (1980).